UDC 629.7.025
DOI: 10.15587/1729-4061.2020.200664

IMPROVING AIRCRAFT FUEL EFFICIENCY BY USING THE ADAPTIVE WING AND WINGLETS

V. Popov
PhD, Chairman of Board
JSC «FED»
Sumska str., 132, Kharkiv, Ukraine, 61023
E-mail: popov@fed.com.ua
V. Loginov
Doctor of Technical Sciences, Senior Researcher
Department of Aircraft Engine Design
National Aerospace University «Kharkiv Aviation Institute»
Chkalova str., 17, Kharkiv, Ukraine, 61070
E-mail: flightpropulsion@gmail.com
V. Shmyrov
PhD, Vice President
Antonov State Enterprise
Tupolieva str, 1, Kyiv, Ukraine, 03062
E-mail: shmyrov@antonov.com
Ye. Ukrainets
Doctor of Technical Sciences, Professor*
E-mail: eukrainez@gmail.com
P. Steshenko
PhD
Research Laboratory of Automated Control Systems
and Target Equipment for Unmanned Aerial Vehicles
State Research Institute of Aviation
Andryushchenko str., 6V, Kyiv, Ukraine, 01135
E-mail: petrstko@ukr.net
P. Hlushchenko
Adjunct
Department of Scientific and Organizational*
E-mail: Glushchenkopa@i.ua
*Department of the Design and
Strength of Aircraft and Engines
Ivan Kozhedub Kharkiv University of Air Force
Sumska str., 77/79, Kharkiv, Ukraine, 61023

Підвищення паливної ефективності літака є однією із основних вимог, які висуваються до перспективних літальних апаратів та літальних апаратів, які модернізуються. Проведено оцінку зміни аеродинамічної якості і, як наслідок, підвищення паливної ефективності дальнього магістрального літака при застосуванні перспективних засобів підвищення аеродинамічної якості. До зазначених засобів відносяться: відмова від механізації кромок крила та від традиційних органів керування шляхом застосування адаптивного крила, штучна ламінарізація течії навколо елементів планеру, застосування кінцевих аеродинамічних поверхонь. Відмова від традиційних органів керування та механізації крила зумовлена необхідністю забезпечення безшовної поверхні елементів планера для запобігання передчасної турбулізації течії і, як наслідок, призводить до зменшення профільного опору літака. Застосування кінцевих аеродинамічних поверхонь направлене на зниження індуктивного опору. Визначення зміни паливної ефективності літака дозволить оцінити зміну його експлуатаційних витрат протягом життєвого циклу.

Дослідження проведено на основі відомого модульного програмного комплексу «Інтеграція 2.1». Інженерно-штурманський розрахунок виконувався для типового профілю польоту дальнього магістрального літака. Показана можливість зменшення витрати палива до 20 %. Найбільший вплив на зменшення витрати палива має ламінарізація течії на поверхні елементів планеру, при цьому зменшення витрати палива склало 17,1 %. Відмова від механізації та елеронів забезпечила зменшення витрати палива на 3,9 %, при цьому відмова від елеронів, передкрилка та закрилка забезпечило зменшення витрати палива на 0,4, 1,5 та 0,4 відсотків відповідно. Застосування спіроїдних кінцевих аеродинамічних поверхонь забезпечило зменшення витрати палива на 1,95 %

Ключові слова: аеродинамічна якість, паливна ефективність, адаптивне крило, штучна ламінарізація, спіроїдні кінцеві аеродинамічні поверхні

Received date 10.02.2020
Accepted date 10.03.2020
Published date 27.04.2020

1. Introduction

Improving the aircraft's (AC) flight and economic characteristics is achieved by improving its aerodynamic characteristics (ACH), the characteristics of its propulsion unit, and by improving the design of the glider using new structural materials and their production technologies [1–3]. A promising direction in modern aircraft engineering is the use of an adaptive wing of the changeable shape and geometry. However, the appropriate adaptive wing mechanization assemblies are needed to implement such a project. The use of energy-efficient electric drives of appropriate dimensions to control adaptive wings would reduce flight weight and optimize the aircraft's characteristics.

A wide range of airfoils is used to control the flight of a modern aircraft. These airfoils are managed by various power drives: hydraulic, pneumatic, and electric. The most promising are electric drives, due to their simplicity of design and efficient mass- size indicators.

The effort required to move an airfoil is determined for each aircraft by surface area, the flight speed, and altitude, as well as other conditions. It should be noted that the bulk of the aircraft's carrier system and steering surfaces is concentrated in power drives. Therefore, it is a relevant scientific and technical task to design simple electromechanical drives with efficient mass-size indicators, which could replace the hydraulic systems. Currently, electric drives are used in systems that control aircraft position and wing mechanization. The wider application of electric drives is limited given the need to ensure the resource and reliability of the electric drive's mechanical part. Among the solutions to this issue, one is to absorb perceived aerodynamic loads in a fixed output link position. Therefore, over the past 10 years, due to the advent of new aircraft materials, there has been increasing attention to the possibility of improving the aerodynamic characteristics of the aircraft based on changing the wing geometry. The wing geometry is modified, depending on the flight mode, by using an adaptive wing.

The possibilities to improve the AC aerodynamic quality have been analyzed, which is an important aerodynamic characteristic that makes it possible to assess the aerodynamic perfection of the aircraft. The aerodynamic quality affects such AC critical competitiveness indicators as cruising speed, the flight range, and duration at a specified payload size [4]. The result of improving the AC aerodynamic quality is the increase in its fuel efficiency. Improving aircraft fuel efficiency is one of the main requirements for advanced and modernized AC. Therefore, it is a relevant task to study the possibilities for improving the AC aerodynamic quality.

2. Literature review and problem statement

The main ways to improve the aerodynamic quality of the prospective and existing AC are stated in [5, 6]. These include reducing the AC drag during flight, active control over flows on the surface of the glider, the use of new structural assemblies. Reducing a drag can be achieved by decreasing the inductive and profile drags. It is possible to reduce inductive drag by increasing the lengthening of the wing and/or the use of winglets (WL) on the wing [5]. Increased lengthening of the wing leads to an increase in the AC size and mass, which is not always acceptable. The effect of the WL use is comparable to an increase in wing lengthening but does not significantly increase the wingspan. It is known that the installation of WL at the correct pairing with the wing leads to a decrease in the end flows, a decrease in the intensity of the end vortex, increases the effective lengthening of the wing, which leads to a decrease in inductive drag. At the same time, it is important to ensure the minimal profile drag of WL and its connection with the wing. At cruising flight modes, the increase in lengthening, which maintains the values of the curving momentum in the root cross-sections of the wing within acceptable limits, provides for a reduction in inductive drag by 10 %. The use of WL reduces inductive resistance by 20 % while maintaining the momentum value within acceptable limits [7]. Therefore, it is advisable to consider the application of WL.

At present, there are a large number of different types of WLs [8]. The most common types of WLs are the Whitcomb's WL, conventional winglets, shark winglets [9]. Studies [10, 11] show that the effectiveness of WL depends on the correct choice of the WL geometric parameters, its spatial position relative to the wing, and the geometric characteristics of the original wing.

At the same time, the most promising ones are the spiroid WLs whose concept is outlined in patent [13]. Papers [14, 15] show significant differences in the distribution of the field of velocities and pressures behind the wing, the structure of the flow when applying spiroid WL in comparison with other types of WL and the wing without WL. A special feature is that several end vortexes form behind the wing with spiroid WLs. The lifespan of the end vortexes and the distance to their fading are the smallest compared to other types of WLs. A numerical study of the effect exerted by the geometric parameters of spiroid WLs on aerodynamic quality, the flight range, and duration of the Falcon 50 aircraft is reported in [16]. Thus, for a simple wing aircraft the maximum flight range was 6,480 km, for a plane with a conventional WL – 6,847 km, and for an aircraft with a spiroid WL – 7,863 km. The maximum flight duration was 6.45 hours, 6.82 hours, 7.83 hours, respectively. The effect of the geometric parameters of spiroid WLs on the long-haul aircraft ACHs was considered in [9]; it was concluded that the spiroids are more effective than conventional WLs at large C_{ya} values. However, due to a large value of the gain in the bending momentum, the study was discontinued because the project was intended to find the WLs that would not require a change in wing design due to the additional bending momentum. Thus, the impact of spiroid WLs on the ACHs of long-haul AC is not fully investigated.

Reducing the AC profile drag is achieved by improving the quality of the streamlined surface, by reducing the number of external add-ons and structural elements, and by using the artificial and natural wing laminarization [17]. Natural laminarization is possible by choosing a favorable distribution of pressure over the wing. However, increasing the size and sweep (up to 20–25°) of the AC wing leads to that the natural laminarization becomes ineffective [17], necessitating the consideration of the artificial laminarization of the flow over the wing surface. One of the techniques of artificial laminarization is to suck the boundary layer off parts of the plane's glider. The effectiveness of a given method was confirmed by experimental studies in wind tunnels [19, 20] and flight tests [21–23]. Paper [19] shows a decrease in the effectiveness of sucking off the boundary layer with an increase in the sweep of the wing model. Study [20] demonstrates a decrease in the effectiveness of sucking off the boundary layer with an increase in the Mach and Reynolds numbers in wind tunnel tests. An overview of AC flight tests with the laminar flow on the surface of the glider elements is given in [21]. Work [22] reports a study into the effect of sucking off the boundary layer in the region where the aircraft wing and fuselage are connected, where the flow is three-dimensional. Under certain conditions at sucking off the boundary layer, the authors observed completely laminar zones of the flow, which, under normal conditions, were turbulent. They also showed the effect exerted on the flow laminarization by the position of a boundary layer suction system relative to the wing root chord. The results of the flight tests of the aircraft with wings with the laminarized compartments in the middle area on the wingspan are described in [23]. The authors revealed a significant impact of irregularities and roughness of the surface in the range of 5 to 20 % of the wing chord on the effectiveness of the boundary layer suction system. In general, when the boundary layer is sucked off, it becomes possible to stretch the laminar regions up to 60–70 % of the wing chord, which would reduce the total drag by 14–15 % [5]. It is promising to suck off the boundary layer in the wing front edge region (about 20 % of the chord) and to implement a favorable negative pressure gradient on most of the AC bearing surface. The presence of the front edge mechanization is an impediment to laminarize the flow.

The emergence of new deformable (flexible) aviation materials makes it possible to consider the wing and mechanization with a solid smooth surface without joints (Fig. 1). The use of an adaptive wing without seams and crevices makes it possible to avoid the surface irregularities, which prevent the flow laminarization. The directions of early research, the challenges and technical difficulties associated with the implementation of the adaptive wing concept, are outlined in [24]. It was shown that along with aerodynamic advantages, the concept of an adaptive wing has a significant disadvantage, namely the increase in the mass of the adaptive wing compared to the conventional wing. An overview of the programs, the levels of technical readiness of modern adaptive wings, is given in [25]. Creating a fully adaptive wing is a complex task and is based on the use of morphing, which implies the possibility of changing the shape or structure of the wing [25]. The shape of the AC adaptive wing is changed by autonomous power drives, including hydraulic, electro hydrostatic, and electromechanical drives with the possibility of incremental and rotational action, which are installed in the adaptive wing (Fig. 2).

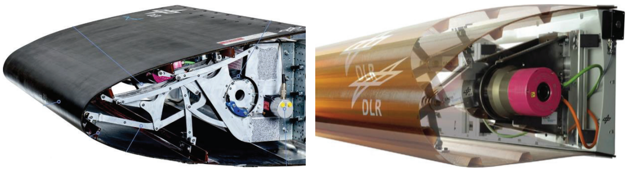

a *b*

Fig. 1. Examples of the adaptive front-end with a drive [27]: *a* — kinematic mechanism; *b* — drive

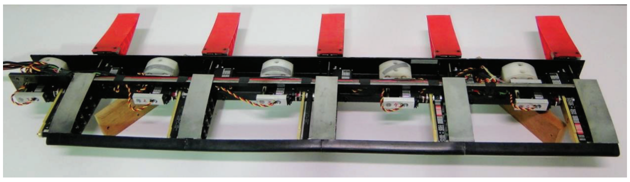

Fig. 2. Example of the design of an adaptive wing with electric drives [28]

Deviating the moving elements while maintaining the smoothness of the contour makes it possible to obtain such a distribution of pressure over the wing surface that prevents the flow detachment or weakens its development under the chosen flight mode [27]. The most advanced technology at present is ACTE (Adaptive Compliant Trailing Edge) [28]. The distinctive feature of a given technology is a deflectable rear edge with a smooth surface without slits. This reduces the wing weight, improves aerodynamic quality and, as a result, reduces fuel consumption, as well as decreases noise during take-off and landing [28, 29]. The wing mass is reduced by decreasing the curving momentum when ACTE is used as the mass of the adaptive flap itself is greater than the mass of the original flap by 4 %.

The studies of the adaptive wing front edge that uses new composite materials are reported in [30, 31]. The aerodynamic optimization of the shape of the adaptive wing tip improves the aerodynamic quality of the wing profile by 1.71 %; the authors also note the difficulty of ensuring the predefined wing tip shape using the retractable kinematics [30]. It is shown in [31] that using a seamless adaptive front edge of the wing makes it possible to increase the maximum lift force coefficient to 8.35 % compared to the wing with a deflectable slit tip. Works [32–34] examined the aerodynamic characteristics of an adaptive wing and compared them with the original wing with conventional mechanization. Abandoning the conventional mechanization of the rear edge in favor of an adaptive wing under the estimated conditions reduces drag by 1 % and by 5 % under other modes [32]. The use of a deflectable rear edge without slits improved the aerodynamic quality of the straight wing section model by 13.6 %, 5.3 %, 5.8 %, and 3.1 % at attack angles of 0, 5, 10, and 15°, respectively, when compared to the wing with the conventional flap [33]. The application of an adaptive wing of the Fish Bone Active Camber concept increases aerodynamic quality by up to 25 % when compared to a wing with a deflectable flap [34]. The results reported in [33, 34] cannot be applied to assess the fuel efficiency of long-haul AC without additional research as the selected models are not suitable for use on long-haul AC.

It should be noted that the above studies do not make it possible to assess the joint impact of the promising means for improving aerodynamic quality on the fuel efficiency of a long-range aircraft. As a result, it is difficult to predict the operating costs of a prospective AC. Hence, it follows that research is needed to determine the joint impact of the promising techniques to improve aerodynamic quality on the AC fuel efficiency during a typical flight profile.

3. The aim and objectives of the study

The aim of this study is to determine a change in aircraft fuel efficiency based on changes in its aerodynamic characteristics. That would make it possible to estimate a decrease in the operating costs during the AC life cycle. In turn, in the future, it could enable determining the permissible costs in the design and application of the concept of an adaptive wing while ensuring the predefined cost level of an aircraft complex.

To accomplish the aim, the following tasks have been set:

– to define a change in the aircraft aerodynamic quality when applying an adaptive wing concept technology;

– to determine a change in aerodynamic quality under the artificial laminarization of the flow over the surface of an AC glider;

– to define a change in aerodynamic quality when using spiroid WLs;

– to determine the impact of ACH change on fuel consumption by a long-range aircraft by performing an engineering and navigational calculation (ENC) for a typical flight profile.

4. Procedure for studying a change in the aerodynamic quality and fuel efficiency when considering the aircraft flight range

We study an aircraft the type of Boeing 747-8 or Airbus A380, representing a four-engine monoplane. In the cross-section, the outer contour of the fuselage is formed by two conjugated circles: at the top, the radius is 1.9 meters; at the bottom, 3.8 meters. The total washed area of the fuselage is 1,500 m^2.

The aircraft wing, with a sweep angle along the quarter line of the chords 27°, is composed of the supercritical profiles of the relative thickness of 13.7 % at the root and 9 % at the endings. The installation angle of the wing is 3.5°, the geometric twist is 3°. The wing uses six-section slats, one-slit three-section flaps of the Fowler type, and four sections of internal, middle, and external interceptors. The internal sections, deflected at an angle of 45°, are designed for braking on the run and interrupted take-off, middle – for braking and emergency reduction on the glissade, external – only for the control of the roll in conjunction with the ailerons.

The empennage is of the regular design, single-keel with the stabilizer, located on the fuselage. The vertical empennage consists of a keel and a turning wheel. The angle of the keel's sweep on the front edge is 40°. The vertical empennage is composed of the profiles of the relative thickness of 12 % at the root and 10 % at its end. The steering wheel deviates at the angles of 25° in both directions.

The horizontal empennage is a controlled stabilizer with a sweep angle at the front edge of 32.75°, fixed, composed of the symmetrical profiles of NACA with a relative thickness of 9.9 % at the root and 7.6 % at its endings. The horizontal empennage ensures static longitudinal stability in the cruising flight over the entire operational range of attack angles except for angles from 9° to 12° when the wing «shadows» the stabilizer.

The power plant includes four turbofan engines with reversing traction devices and two auxiliary propulsion systems.

Our study employed the methods of mathematical modeling of the process of flowing around the surface of the glider and its elements, general scientific methods of analysis and synthesis. A semi-empirical method was used to obtain the main aerodynamic characteristics of the aircraft and perform the engineering and navigational calculation of the aircraft's flight.

We studied the characteristics of a long-range heavy aircraft under conditions of a typical flight profile using the developed modular software complex «Integration-2.1» (Fig. 3, 4), based on the methodology outlined in works [35–37].

The modular software complex was developed to conduct parametric studies of the aircraft's operational characteristics during its modernization or pre-design phases. The modular complex includes the following software units:

– the initial technical and economic data on the propulsion engine of the propulsion system and its possible prototype;

– the initial data on AC's flight, technical and economic characteristics;

– the source geometric data on the engine with a moto nacelle and the elements of the aircraft glider;

– the adjustment of an AC weight balance;

– the initial data on the typical flight profile of the aircraft;

– the calculation of the AC aerodynamic characteristics;

– the calculation of the AC flight-technical, weight, and flight characteristics;

– the calculation of the price of the main engine and an auxiliary propulsion system;

– the calculation of the need for engines, overhaul and ongoing repairs under the chosen maintenance and repair strategy;

– the calculation of the cost of the aircraft's glider life cycle;

– the calculation of the cost of the life cycle of a power plant engine;

– the calculation of AC's economic performance;

– reporting on the AC project.

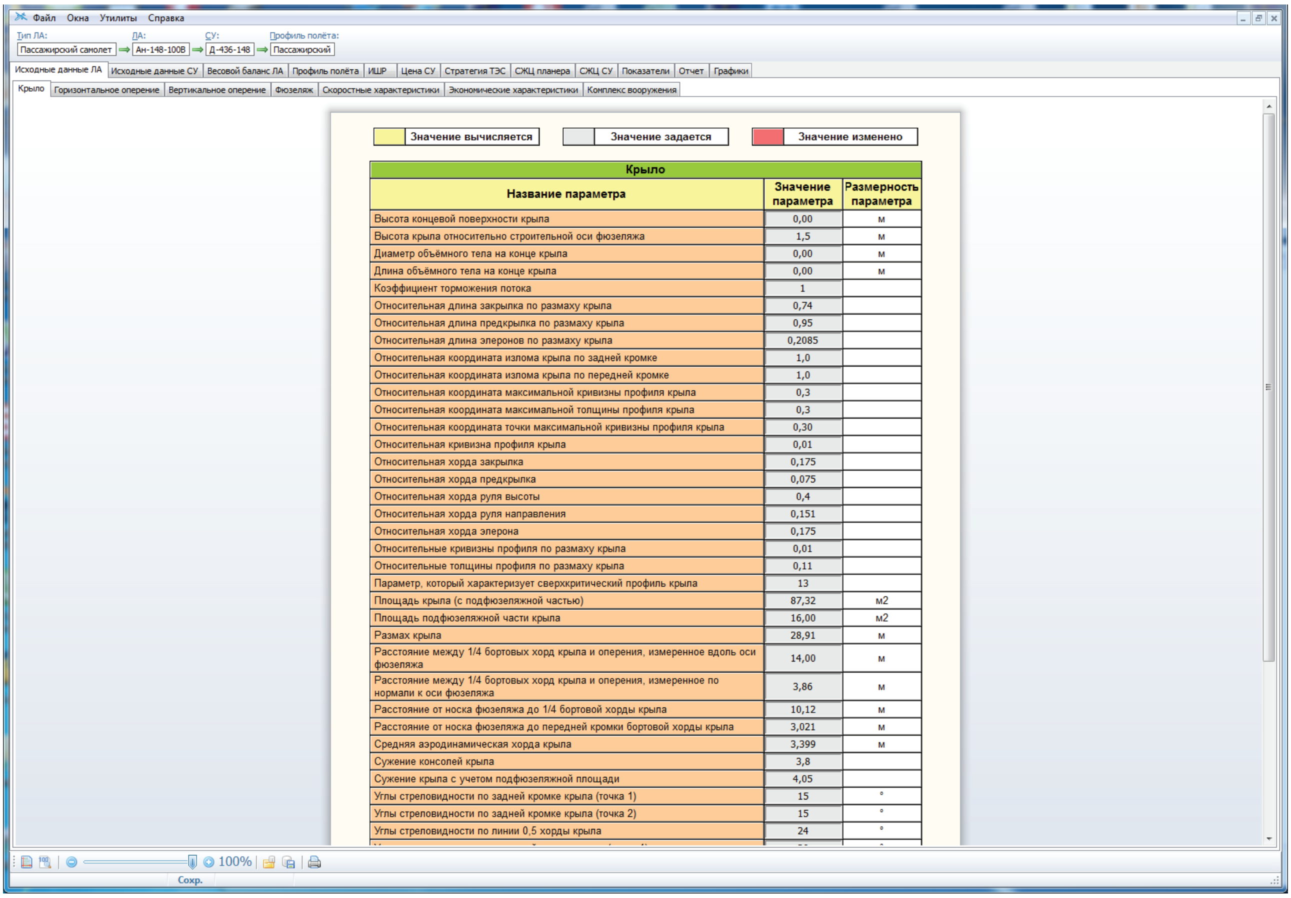

Тип ЛА: Пассажирский самолет ⇒ ЛА: Ан-148-100В ⇒ СУ: Д-436-148 ⇒ Профиль полёта: Пассажирский

🟨 Значение вычисляется
⬜ Значение задается
🟥 Значение изменено

Крыло		
Название параметра	**Значение параметра**	**Размерность параметра**
Высота концевой поверхности крыла	0,00	м
Высота крыла относительно строительной оси фюзеляжа	1,5	м
Диаметр объёмного тела на конце крыла	0,00	м
Длина объёмного тела на конце крыла	0,00	м
Коэффициент торможения потока	1	
Относительная длина закрылка по размаху крыла	0,74	
Относительная длина предкрылка по размаху крыла	0,95	
Относительная длина элеронов по размаху крыла	0,2085	
Относительная координата излома крыла по задней кромке	1,0	
Относительная координата излома крыла по передней кромке	1,0	
Относительная координата максимальной кривизны профиля крыла	0,3	
Относительная координата максимальной толщины профиля крыла	0,3	
Относительная координата точки максимальной кривизны профиля крыла	0,30	
Относительная кривизна профиля крыла	0,01	
Относительная хорда закрылка	0,175	
Относительная хорда предкрылка	0,075	
Относительная хорда руля высоты	0,4	
Относительная хорда руля направления	0,151	
Относительная хорда элерона	0,175	
Относительные кривизны профиля по размаху крыла	0,01	
Относительные толщины профиля по размаху крыла	0,11	
Параметр, который характеризует сверхкритический профиль крыла	13	
Площадь крыла (с подфюзеляжной частью)	87,32	м2
Площадь подфюзеляжной части крыла	16,00	м2
Размах крыла	28,91	м
Расстояние между 1/4 бортовых хорд крыла и оперения, измеренное вдоль оси фюзеляжа	14,00	м
Расстояние между 1/4 бортовых хорд крыла и оперения, измеренное по нормали к оси фюзеляжа	3,86	м
Расстояние от носка фюзеляжа до 1/4 бортовой хорды крыла	10,12	м
Расстояние от носка фюзеляжа до передней кромки бортовой хорды крыла	3,021	м
Средняя аэродинамическая хорда крыла	3,399	м
Сужение консолей крыла	3,8	
Сужение крыла с учетом подфюзеляжной площади	4,05	
Углы стреловидности по задней кромке крыла (точка 1)	15	°
Углы стреловидности по задней кромке крыла (точка 2)	15	°
Углы стреловидности по линии 0,5 хорды крыла	24	°

Fig. 3. User dialogue window «AC initial data – Wing»

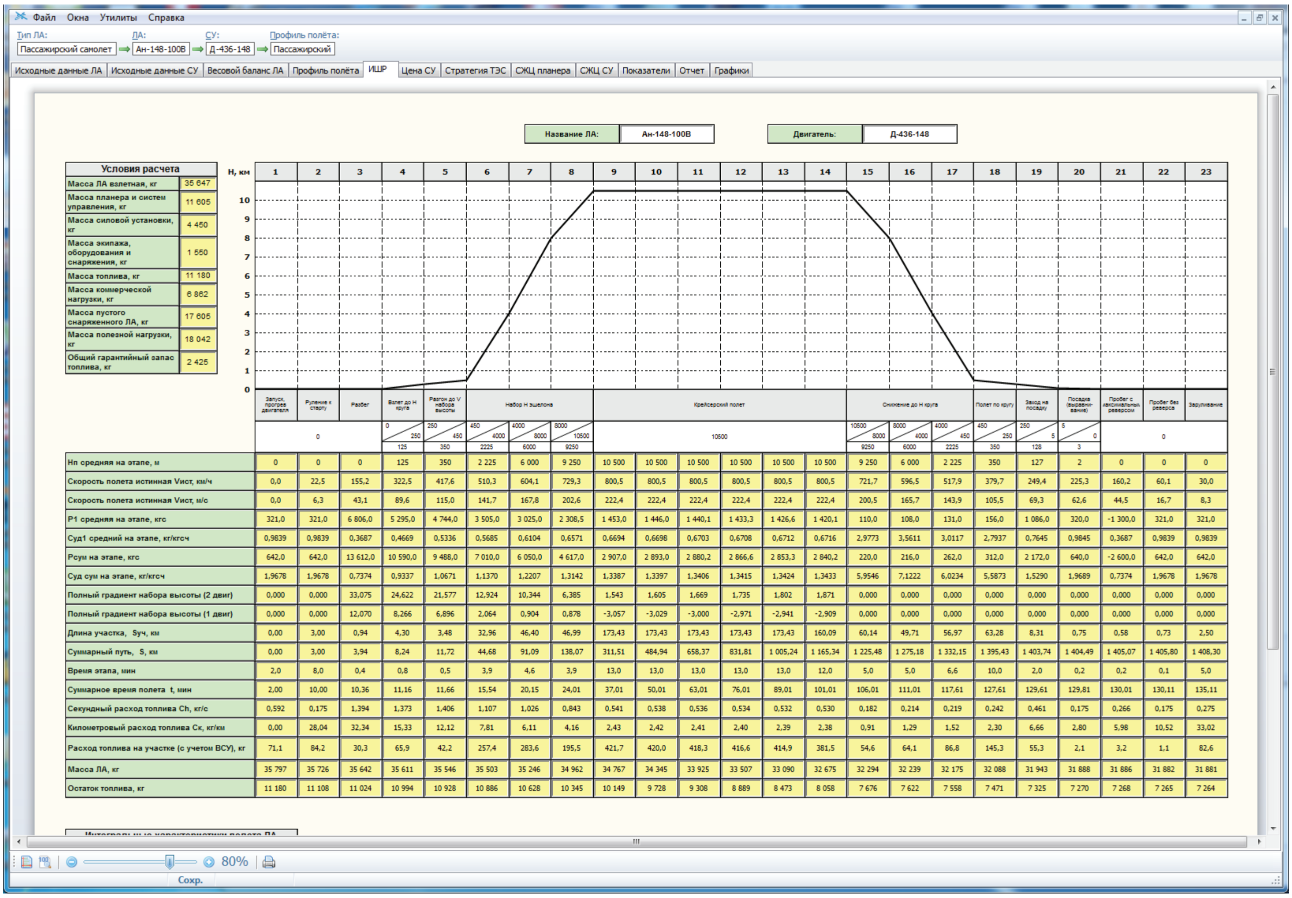

Тип ЛА: Пассажирский самолет
ЛА: Ан-148-100В
СУ: Д-436-148
Профиль полёта: Пассажирский

Название ЛА: Ан-148-100В
Двигатель: Д-436-148

Условия расчета	
Масса ЛА взлетная, кг	35 647
Масса планера и систем управления, кг	11 605
Масса силовой установки, кг	4 450
Масса экипажа, оборудования и снаряжения, кг	1 550
Масса топлива, кг	11 180
Масса коммерческой нагрузки, кг	6 862
Масса пустого снаряженного ЛА, кг	17 605
Масса полезной нагрузки, кг	18 042
Общий гарантийный запас топлива, кг	2 425

Н, км	1	2	3	4	5	6	7	8	9	10	11	12	13	14	15	16	17	18	19	20	21	22	23
	Запуск, прогрев двигателя	Руление к старту	Разбег	Взлет до Н круга	Разгон до V набора высоты	Набор Н эшелона			Крейсерский полет						Снижение до Н круга			Полет по кругу	Заход на посадку	Посадка (выравни-вание)	Пробег с максимальным реверсом	Пробег без реверса	Заруливание
	0			0 250 125	250 450 350	450 4000 2225	4000 8000 6000	8000 10500 9250	10500						10500 8000 9250	8000 4000 6000	4000 450 2225	450 250 350	250 5 128	5 0 3	0		
Нп средняя на этапе, м	0	0	0	125	350	2 225	6 000	9 250	10 500	10 500	10 500	10 500	10 500	10 500	9 250	6 000	2 225	350	127	2	0	0	0
Скорость полета истинная Vист, км/ч	0,0	22,5	155,2	322,5	417,6	510,3	604,1	729,3	800,5	800,5	800,5	800,5	800,5	800,5	721,7	596,5	517,9	379,7	249,4	225,3	160,2	60,1	30,0
Скорость полета истинная Vист, м/с	0,0	6,3	43,1	89,6	115,0	141,7	167,8	202,6	222,4	222,4	222,4	222,4	222,4	222,4	200,5	165,7	143,9	105,5	69,3	62,6	44,5	16,7	8,3
Р1 средняя на этапе, кгс	321,0	321,0	6 806,0	5 295,0	4 744,0	3 505,0	3 025,0	2 308,5	1 453,0	1 446,0	1 440,1	1 433,3	1 426,6	1 420,1	110,0	108,0	131,0	156,0	1 086,0	320,0	-1 300,0	321,0	321,0
Суд1 средний на этапе, кг/кгсч	0,9839	0,9839	0,3687	0,4669	0,5336	0,5685	0,6104	0,6571	0,6694	0,6698	0,6703	0,6708	0,6712	0,6716	2,9773	3,5611	3,0117	2,7937	0,7645	0,9845	0,3687	0,9839	0,9839
Рсум на этапе, кгс	642,0	642,0	13 612,0	10 590,0	9 488,0	7 010,0	6 050,0	4 617,0	2 907,0	2 893,0	2 880,2	2 866,6	2 853,3	2 840,2	220,0	216,0	262,0	312,0	2 172,0	640,0	-2 600,0	642,0	642,0
Суд сум на этапе, кг/кгсч	1,9678	1,9678	0,7374	0,9337	1,0671	1,1370	1,2207	1,3142	1,3387	1,3397	1,3406	1,3415	1,3424	1,3433	5,9546	7,1222	6,0234	5,5873	1,5290	1,9689	0,7374	1,9678	1,9678
Полный градиент набора высоты (2 двиг)	0,000	0,000	33,075	24,622	21,577	12,924	10,344	6,385	1,543	1,605	1,669	1,735	1,802	1,871	0,000	0,000	0,000	0,000	0,000	0,000	0,000	0,000	0,000
Полный градиент набора высоты (1 двиг)	0,000	0,000	12,070	8,266	6,896	2,064	0,904	0,878	-3,057	-3,029	-3,000	-2,971	-2,941	-2,909	0,000	0,000	0,000	0,000	0,000	0,000	0,000	0,000	0,000
Длина участка, Sуч, км	0,00	3,00	0,94	4,30	3,48	32,96	46,40	46,99	173,43	173,43	173,43	173,43	173,43	160,09	60,14	49,71	56,97	63,28	8,31	0,75	0,58	0,73	2,50
Суммарный путь, S, км	0,00	3,00	3,94	8,24	11,72	44,68	91,09	138,07	311,51	484,94	658,37	831,81	1 005,24	1 165,34	1 225,48	1 275,18	1 332,15	1 395,43	1 403,74	1 404,49	1 405,07	1 405,80	1 408,30
Время этапа, мин	2,0	8,0	0,4	0,8	0,5	3,9	4,6	3,9	13,0	13,0	13,0	13,0	13,0	12,0	5,0	5,0	6,6	10,0	2,0	0,2	0,2	0,1	5,0
Суммарное время полета t, мин	2,00	10,00	10,36	11,16	11,66	15,54	20,15	24,01	37,01	50,01	63,01	76,01	89,01	101,01	106,01	111,01	117,61	127,61	129,61	129,81	130,01	130,11	135,11
Секундный расход топлива Ch, кг/с	0,592	0,175	1,394	1,373	1,406	1,107	1,026	0,843	0,541	0,538	0,536	0,534	0,532	0,530	0,182	0,214	0,219	0,242	0,461	0,175	0,266	0,175	0,275
Километровый расход топлива Ск, кг/км	0,00	28,04	32,34	15,33	12,12	7,81	6,11	4,16	2,43	2,42	2,41	2,40	2,39	2,38	0,91	1,29	1,52	2,30	6,66	2,80	5,98	10,52	33,02
Расход топлива на участке (с учетом ВСУ), кг	71,1	84,2	30,3	65,9	42,2	257,4	283,6	195,5	421,7	420,0	418,3	416,6	414,9	381,5	54,6	64,1	86,8	145,3	55,3	2,1	3,2	1,1	82,6
Масса ЛА, кг	35 797	35 726	35 642	35 611	35 546	35 503	35 246	34 962	34 767	34 345	33 925	33 507	33 090	32 675	32 294	32 239	32 175	32 088	31 943	31 888	31 886	31 882	31 881
Остаток топлива, кг	11 180	11 108	11 024	10 994	10 928	10 886	10 628	10 345	10 149	9 728	9 308	8 889	8 473	8 058	7 676	7 622	7 558	7 471	7 325	7 270	7 268	7 265	7 264

Fig. 4. User dialogue window «Engineering and navigational calculation»

In the software complex, local sources of the additional aircraft drag include small structural elements and add-ons protruding into the flow (antennas, brackets and suspension nodes, PVD tubes, fairings).

The irregularities and joints of the cladding sheets, the cracks on the wing in the location of the mechanization or controls on the empennage also belong to the local sources of additional drag. It is believed that by their nature the local drags are almost independent of the angles of attack. In the overall balance of aircraft drag, the local drags can reach up to 20 % of the original value. Therefore, one of the ways to reduce the aircraft drag is to improve the quality of the streamlined surface, reduce the number of external add-ons and structural elements, perform other design and technological activities.

To eliminate errors related to determining the areas of small elements, the data on their drag is represented in the form of a product $\Delta(C_xS)$. The desired values of drag coefficients are derived from dividing $\Delta(C_xS)$ by the characteristic area: $\Delta C_x=\Delta(C_xS)/S$. Table 1 gives data on the drag coefficients for the most characteristic elements of the aircraft's design.

If necessary, additional drag can be taken into consideration for the engine nozzle with a noise jamming system $\Delta C_x=0.025\,n\,(S_{nozzle}/S)$, where n is the number of engines, S_{nozzle} is the area of the nozzle output cross-section.

When calculating the flight range, duration, and fuel reserve, the following is considered:

– the fuel consumed on the launch, engine testing, and steering ($m_{f.earth}$);

– the fuel consumed on take-off ($m_{f.take\text{-}off}$) – 1,420 kg;

– the fuel consumed for a set of aircraft altitude;

– the fuel consumed on a horizontal flight section;

– the fuel used when descending the height of the echelon to the height of the circle (400...500 m);

– the warranted fuel reserve (aeronautical and compensatory);

– the non-used fuel – 1,200 kg.

Table 1

The $\Delta(C_xS)$ values for the most characteristic elements of the aircraft's design

The aircraft characteristic element	Drag coefficient value
Antenna	0.0015
Fairing of the suspension unit for controls and mechanization	0.0004
A node of the outer suspension holder	0.0004
PVD tube	0.0008
Anti-icing system sensor	0.0012
Aeronautical lights	0.0016
Suction and exhaust pipes	0.0021

It should be noted that the applied procedure for determining the main aerodynamic characteristics produces somewhat inflated values of the aircraft drag, which is necessary to take into consideration the deterioration in the aircraft aerodynamic characteristics during actual operation, to compensate for the difference between the estimated characteristics of the engines and the real ones.

5. Results of studying a change in the AC aerodynamic quality and fuel efficiency

5. 1. The change in aerodynamic quality when applying promising tools to reduce the aircraft drag

Based on the results of our study, obtained by employing the «Integration-2.1» software complex, we derived the dependences (Fig. 5) of the gain in aerodynamic quality on the aircraft's lift force coefficient $\Delta K(C_{ya})$ using the adaptive wing concept when compared to the original aircraft. The seamless mechanization and rudders imply the use of the flexible cladding and drives for a deflected part. The prospective aircraft implies the application of flow laminarization on the surface of the wing, the seamless mechanization and aircraft rudders, and a spiroid-type WL.

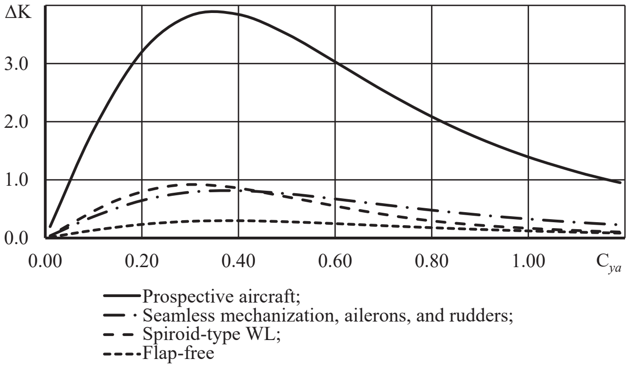

Fig. 5. Gain in aerodynamic quality K due to the lift force coefficient C_{ya} when applying promising technologies

5. 2. Effect of the aerodynamic quality change on fuel consumption when a heavy aircraft flight range is examined

The results of calculating the fuel residue for the cruising flight of the prospective aircraft are given in Table 2. Such representation makes it possible to quantify the actual fuel consumption at major flight sections.

The starting condition corresponds to the refueled aircraft before the flight. The take-off and altitude phases take into consideration fuel consumption for the launch, warming, and steering of the aircraft. The fuel consumption corresponding to take-off is considered to be pre-assigned. Fuel consumption for the height setting of the echelon, in this case, is calculated without intermediate stages. Cruise flight modes correspond to the estimated conditions. To improve fuel economy, it is advisable to adjust C_{ya} as often as possible, as the fuel is consumed, especially at the beginning of the cruising phase of the flight. In our calculations, C_{ya} at cruising is adjusted once. The descent stage is performed without flying in the waiting area.

Our fuel economy estimation, when using the considered modernization tools, is shown in Fig. 6. Such representation makes it possible to estimate a gain from each means of improving the aerodynamic quality.

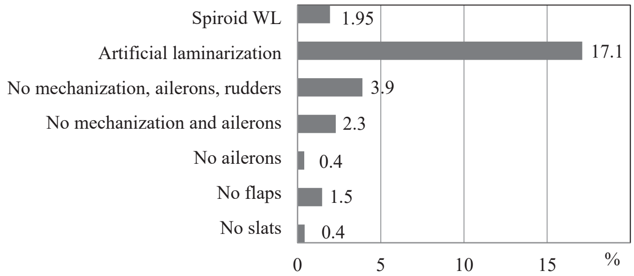

Fig. 6. A decrease in fuel consumption by the modified aircraft compared to the original aircraft

The largest reduction in fuel consumption is provided by the artificial laminarization of the flow on the surface of the aircraft glider. This is a consequence of the decrease in the AC profile drag and the effectiveness over the entire range of attack angles. The winglets allow for substantial fuel economy as they are most efficient under a cruising flight mode. For a typical long-distance AC flight profile, these sections are the longest.

Table 2

Results of fuel consumption calculation for a typical flight profile

Parameter	Flight stages					
	Starting condition	Takeoff, climb	Flight cruising modes		De-scent	Landing, steering
Section length, km	–	270	3,886	4,402	120	–
Total length, km	–	270	4,156	8,558	8,678	8,678
Speed, km/h	–	–	475	475	–	–
Air speed, km/h	–	–	750	750	–	–
Flight duration over a section, min	–	25	311	352	11	15
Total flight duration, min	–	25	336	688	699	714
Hourly fuel consumption, kg/h	–	–	11,190	9,934	–	–
Specific flight range, km/kg	–	–	0.067	0.0755	–	–
Fuel consumption over a section, kg	–	9,800	58,000	58,300	1,000	4,100
Fuel residue, kg	153,000	143,200	85,200	26,900	25,900	21,800
Aircraft mass, kg	355,000	345,200	287,200	228,900	227,900	223,800

6. Discussion of results of estimating the change in the aerodynamic quality and fuel efficiency

When upgrading an aircraft, the abandonment of conventional slats and ailerons in favor of an adaptive wing ensures an increase in the maximum aerodynamic quality $K_{\max}$ by 0.36 % and 0.35 %, respectively, which is the lowest indicator. The abandonment of the flaps provides for a 1.3 % increase in $K_{\max}$, which is due to the greater area relative to the ailerons and the slat. The greatest contribution to the gain in aerodynamic quality, compared to the original aircraft, is ensured by the artificial laminarization of the flow over the wing surface. A growth in $K_{\max}$ due to artificial laminarization was 15.6 %. In total, when using all the tools considered, the increase in $K_{\max}$ was 20.5 %. Abandoning a conventional slat is one of the key stages in the application of flow laminarization tools, despite the small increase in the aerodynamic quality and reduced consumption compared to the abandonment of other types of mechanization. A significant advantage of a given approach is the reduction of AC drag under all flight modes.

However, reducing the profile drag allows for a greater increase in the aerodynamic quality over a certain range of C_{ya} values, despite the effectiveness over the entire range of attack angles. As a C_{ya} value increases, the share of the inductive component of the frontal drag is increased. The profile drag of the glider remains almost constant while the gain in aerodynamic quality decreases.

WL ensures a reduction in inductive drag, which is caused by the presence of a lift force and is associated with the formation of a vortex flow structure in the trail of the aircraft [38]. The use of spiroid WLs reduces the intensity of end vortexes, as do other types of WLs. Significant is the change in the velocity field in the region behind the end of the wing and the erosion of the end vortex (Fig. 7). This change in the velocity field reduces the downwash in front of the wing and improves the aerodynamic quality of the aircraft's wing.

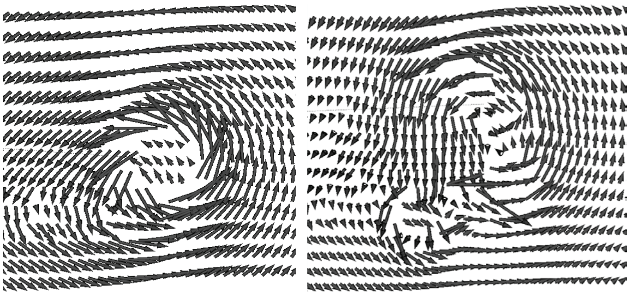
a *b*

Fig. 7. Comparison of the velocity field behind the end of the wing without WL and with the spiroid WL: *a* — wing without WL; *b* — wing with a spiroid type WL

The use of WL provides an increase in the aerodynamic quality over a certain range of C_{ya}. This is due to the fact that at low C_{ya} values the share of inductive drag in the overall drag is small. As a result, the WL's own introduced profile drag prevails over the gain in inductive drag. The increase in C_{ya} enhances the role of inductive drag. The gain in the inductive drag of the assembly wing–WL prevails over the WL profile drag. As C_{ya} continues to grow, there are changes in the spatial flow structure near the ends of the wing, thereby WLs begin to lose their effectiveness.

Thus, we have derived the dependences of change in the aerodynamic quality of a long-range aircraft in the joint and separate application of the promising means of aerodynamic quality enhancement (Fig. 5). The increase in aerodynamic quality is achieved by reducing the components of frontal drag: profile and inductive drag. Profile drag is reduced by laminarizing the flow, eliminating the protrusions and irregularities at the surface of the glider elements. The use of WL, due to the change in the vortex structure behind the wing (Fig. 7), has made it possible to reduce the inductive component of the frontal drag.

We estimated a change in the AC fuel efficiency by carrying out the engineering and navigational calculation for a typical flight profile of a long-range aircraft. The reduction in fuel consumption (Fig. 6) reaches 22.9 % and is the limit for a given type of aircraft. The ENC did not take into consideration the additional balance losses due to the change in the distribution of pressure over the surface of the glider. In addition, the energy costs for sucking off the boundary layer and the operation of units that enable the movement of the kinematics of the adaptive wing were not taken into consideration.

Since artificial laminarization provides the greatest fuel economy, the most promising are studies aimed at ensuring the steady laminar flow around the glider under all flight modes.

7. Conclusions

1. It has been shown that the application of the adaptive wing technology improves aerodynamic quality by eliminating the local sources of drag. Abandoning the slat and aileron in favor of an adaptive wing ensures an increase in $K_{\max}$ by 0.36 % and 0.35 %, respectively, which is the lowest indicator. The abandonment of the flaps provides for a 1.3 % increase in $K_{\max}$, which is due to the greater area relative to the ailerons and the slat.
2. It has been established that the most effective method of increasing aerodynamic quality is the laminarization of the flow over the surface of the aircraft glider. The maximum aerodynamic gain was 15.6 % relative to the original aircraft. The advantage of a given approach is a decrease in the profile drag under all flight modes.
3. It has been demonstrated that the spiroid WLs ensure the greatest reduction in inductive drag at C_{ya} close to cruising values. The increase in the maximum aerodynamic quality was 1.9 % compared to the aircraft without WL.
4. It has been established that the best way to improve the aircraft fuel efficiency is to artificially laminarize the flow over the surface of the glider. Implementation of such a solution without taking into consideration the energy costs for sucking off the boundary layer would amount to 17.1 % fuel economy. Abandoning the slat is one of the less effective methods of reducing fuel consumption, however, without such a solution, the implementation of flow laminarization would be difficult. The joint application of the considered advanced means of improving aerodynamic quality on a promising long-haul aircraft would provide a 22.9 % fuel economy. The results obtained allow us to estimate the reduction in operating costs and determine the permissible costs in the development and application of the concept of an adaptive wing while ensuring the predefined cost level of an aircraft complex.

References

1. Arutyunov, A. G., Dydyshko, D. V., Endogur, A. I., Kuznetsov, K. V., Tolmachev, V. I. (2016). Perspektivy razvitiya transportnyh samoletov. Trudy MAI, 90. Available at: https://mai.ru/upload/iblock/d01/arutyunov_dydyshko_endogur_kuznetsov_tolmachev_rus2_1.pdf

2. Levickiy, S. V., Levickaya, E. V. (2014). The methods of assessment of transportation efficiency of a passenger aircraft. Nauchniy vestnik MGTU GA, 205, 99–106. Available at: https://avia.mstuca.ru/jour/article/view/636/554
3. Ruban, I., Khudov, H., Makoveichuk, O., Khizhnyak, I., Khudov, V., Podlipaiev, V. et. al. (2019). Segmentation of optical-electronic images from on-board systems of remote sensing of the earth by the artificial bee colony method. Eastern-European Journal of Enterprise Technologies, 2 (9 (98)), 37–45. doi: https://doi.org/10.15587/1729-4061.2019.161860
4. Tinyakov, D. V. (2013). Vliyanie chastnyh kriteriev effektivnosti nesushchih poverhnostey samoletov transportnoy kategorii na velichinu kreyserskogo aerodinamicheskogo kachestva. Voprosy proektirovaniya i proizvodstva konstruktsiy letatel'nyh apparatov, 2, 18–24. Available at: http://nbuv.gov.ua/UJRN/Pptvk_2013_2_4
5. Benzakein, M. J. (2014). What does the future bring? A look at technologies for commercial aircraft in the years 2035–2050. Propulsion and Power Research, 3 (4), 165–174. doi: https://doi.org/10.1016/j.jppr.2014.11.004
6. Abbas, A., de Vicente, J., Valero, E. (2013). Aerodynamic technologies to improve aircraft performance. Aerospace Science and Technology, 28 (1), 100–132. doi: https://doi.org/10.1016/j.ast.2012.10.008
7. Jucobs, P. F., Flechner, S. G., Montoya, L. C. (1977). Effect of winglets on a first-generation jet transport wing. I – longitudinal aerodynamic characteristics of a semispan model at subsonic speeds. NASA technical note. Wishington, D-8473, 48. Available at: https://ntrs.nasa.gov/archive/nasa/casi.ntrs.nasa.gov/19780012121.pdf
8. Djojodihardjo, H. (2011). Review on Development and Recent Patents on Trailing Vortices Alleviation. Recent Patents on Mechanical Engineeringe, 4 (2), 83–129. doi: https://doi.org/10.2174/2212797611104020083
9. Hantrais-Gervois, J.-L., Grenon, R., Mann, A., Büscher, A. (2009). Downward pointing winglet design and assessment within the M-DAW research project. The Aeronautical Journal, 113 (1142), 221–232. doi: https://doi.org/10.1017/s000192400000289x
10. Whitcomb, R. T. (1976). A design approach and selected wind-tunnel results at high subsonic speeds for wing-tip mounted. NASA technical note, D-8260, 30. Available at: https://ntrs.nasa.gov/archive/nasa/casi.ntrs.nasa.gov/19760019075.pdf
11. Céron-Muñoz, H. D., Cosin, R., Coimbra, R. F. F., Correa, L. G. N., Catalano, F. M. (2013). Experimental Investigation of Wing-Tip Devices on the Reduction of Induced Drag. Journal of Aircraft, 50 (2), 441–449. doi: https://doi.org/10.2514/1.c031862
12. International Air Transport Association IATA (2013). IATA Technology Roadmap.
13. Gratzer, L. B. (1991). Pat. No. US5102068A. Spiroid-tipped wing. No. 660,651; declareted: 25.02.91; published: 7.04.92. Available at: https://patentimages.storage.googleapis.com/bb/2c/14/e925d497e132fa/US5102068.pdf
14. Nazarinia, M., Soltani, M. R., Ghorb, K. (2006). Experimental study of vortex shapes behind a wing equipped with different winglets. JAST, 3 (1), 1–15. Available at: https://www.sid.ir/FileServer/JE/99120060101.pdf
15. Guerrero, J. E., Maestro, D., Bottaro, A. (2012). Biomimetic spiroid winglets for lift and drag control. Comptes Rendus Mécanique, 340 (1-2), 67–80. doi: https://doi.org/10.1016/j.crme.2011.11.007
16. Mostafa, S., Bose, S., Nair, A., Raheem, M. A., Majeed, T., Mohammed, A., Kim, Y. (2014). A parametric investigation of non-circular spiroid winglets. EPJ Web of Conferences, 67, 02077. doi: https://doi.org/10.1051/epjconf/20146702077
17. Catalin, N. (2014). Advanced Aerodynamic Technologies for Future Green Regional Aircraft. INCAS BULLETIN, 6 (Special 1), 99–110. doi: https://doi.org/10.13111/2066-8201.2014.6.s1.11
18. Bushnell, D. M., Malik, M. R. (1987). Application of Stability Theory to Laminar Flow Control – Progress and Requirements. Stability of Time Dependent and Spatially Varying Flows, 1–17. doi: https://doi.org/10.1007/978-1-4612-4724-1_1
19. Chernyshev, S. L., Kiselev, A. P., Kuryachii, A. P. (2011). Laminar flow control research at TsAGI: Past and present. Progress in Aerospace Sciences, 47 (3), 169–185. doi: https://doi.org/10.1016/j.paerosci.2010.11.001
20. Bokser, V. D., Babuev, V., Kiselev, A., Mikeladze, V. G., Shapovalov, G. K. (1997). The Experimental Investigation of HLFC-System Use on the Swept Wing at Subsonic Velocities. SAE Technical Paper Series. doi: https://doi.org/10.4271/975500
21. Collier, F. S. (1994). Recent progress in the development of laminar flow aircraft. ICAS Proceedings, 3 (19), 2436–2455. Available at: https://www.icas.org/ICAS_ARCHIVE/ICAS1994/ICAS-94-4.7.1.pdf
22. Horstmann, K., Redeker, G., Quast, A., Dressler, U., Bieler, H. (1990). Flight tests with a natural laminar flow glove on a transport aircraft. Flight Simulation Technologies Conference and Exhibit. doi: https://doi.org/10.2514/6.1990-3044
23. Bulgubre, C., Arnal, D. (1992). Dassault Falcon 50 laminar flow flight demonstrator. Proceedings First European Forum on Laminar Flow Technology. Hamburg, 11–19.
24. Barbarino, S., Bilgen, O., Ajaj, R. M., Friswell, M. I., Inman, D. J. (2011). A Review of Morphing Aircraft. Journal of Intelligent Material Systems and Structures, 22 (9), 823–877. doi: https://doi.org/10.1177/1045389x11414084
25. Li, D., Zhao, S., Da Ronch, A., Xiang, J., Drofelnik, J., Li, Y. et. al. (2018). A review of modelling and analysis of morphing wings. Progress in Aerospace Sciences, 100, 46–62. doi: https://doi.org/10.1016/j.paerosci.2018.06.002
26. Kiselev, M. A., Ismagilov, F. R., Vavilov, V. E., Sayakhov, I. F. (2017). Problem of adaptive wings applicalion. Vestnik UGATU, 21 (1 (75)), 136–141. Available at: http://journal.ugatu.ac.ru/index.php/Vestnik/article/view/29
27. Thill, C., Etches, J., Bond, I., Potter, K., Weaver, P. (2008). Morphing skins. The Aeronautical Journal, 112 (1129), 117–139. doi: https://doi.org/10.1017/s0001924000002062

28. Kota, S., Flick, P., Collier, F. S. (2016). Flight Testing of FlexFloilTM Adaptive Compliant Trailing Edge. 54th AIAA Aerospace Sciences Meeting. doi: https://doi.org/10.2514/6.2016-0036
29. Sodja, J., Martinez, M. J., Simpson, J. C., De Breuker, R. (2015). Experimental Evaluation of the Morphing Leading Edge Concept. 23rd AIAA/AHS Adaptive Structures Conference. doi: https://doi.org/10.2514/6.2015-0791
30. Magrini, A., Benini, E. (2018). Aerodynamic Optimization of a Morphing Leading Edge Airfoil with a Constant Arc Length Parameterization. Journal of Aerospace Engineering, 31 (2), 04017093. doi: https://doi.org/10.1061/(asce)as.1943-5525.0000812
31. Magrini, A., Benini, E., Ponza, R., Wang, C., Khodaparast, H., Friswell, M. et. al. (2019). Comparison of Constrained Parameterisation Strategies for Aerodynamic Optimisation of Morphing Leading Edge Airfoil. Aerospace, 6 (3), 31. doi: https://doi.org/10.3390/aerospace6030031
32. Lyu, Z., Martins, J. R. R. A. (2015). Aerodynamic Shape Optimization of an Adaptive Morphing Trailing-Edge Wing. Journal of Aircraft, 52 (6), 1951–1970. doi: https://doi.org/10.2514/1.c033116
33. Ninian, D., Dakka, S. (2017). Design, Development and Testing of Shape Shifting Wing Model. Aerospace, 4 (4), 52. doi: https://doi.org/10.3390/aerospace4040052
34. Woods, B. K. S., Bilgen, O., Friswell, M. I. (2012). Wind Tunnel Testing of the Fish Bone Active Camber Morphing Concept. ICAST, 54, 1–14. Available at: http://michael.friswell.com/PDF_Files/C332.pdf
35. Loginov, V. V., Ukrainetc, E. A., Kravchenko, I. F., Yelanskiy, A. V. (2014). Engineering-and-economical performance estimation methodic of a light domestic airliner – turboprop engine system. Systemy ozbroiennia i viyskova tekhnika, 1 (37), 150–160.
36. Loginov, V. V., Kravchenko, I. F., Elanskiy, A. V., Smyk, S. I. (2012). Uluchshenie letno-tehnicheskih harakteristik uchebno-trenirovochnogo samoleta na osnove vybora i zameny dvigatelya silovoy ustanovki. Systemy ozbroiennia i viyskova tekhnika, 1 (29), 60–67. Available at: http://www.hups.mil.gov.ua/periodic-app/article/1943/soivt_2012_1_16.pdf
37. Loginov, V., Ukraintes, Y. (2016). Analysis of operational characteristics of aviation dieseland gas turbine engines for light passenger aircraft. Transactions of the Institute of Aviation, 245 (4), 103–115. doi: https://doi.org/10.5604/05096669.1226429
38. Petrov, A. S. (2009). Podemnaya sila i induktivnoe soprotivlenie kryla konechnogo razmaha v potoke vyazkogo szhimaemogo gaza pri dozvukovyh skorostyah. Uchenye zapiski TSAGI, 5, 16–28. Available at: https://cyberleninka.ru/article/n/podemnaya-sila-i-induktivnoe-soprotivlenie-kryla-konechnogo-razmaha-v-potoke-vyazkogo-szhimaemogo-gaza-pri-dozvukovyh-skorostyah